

pubs.acs.org/Macromolecules Article

Exploring the Potential of Triphenylmethane-Based Polymers Prepared via Facile Friedel—Craft (F—C) Hydroxyalkylation Polymerization as Gas Separation Membranes: Effect of Substituent Group

Mengdi Liu,[§] Andrew Trowbridge,[§] Alexander Hymes, Haifeng Gao,* and Ruilan Guo*



Cite This: Macromolecules 2024, 57, 8202-8211



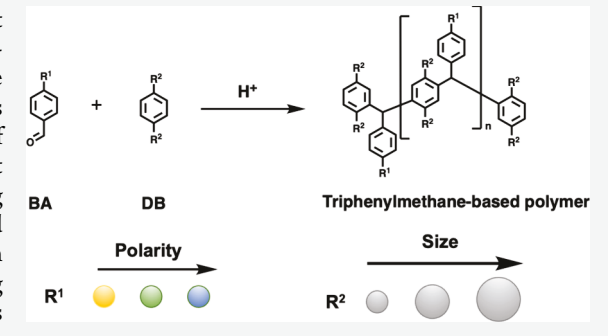
ACCESS

III Metrics & More

Article Recommendations

Supporting Information

ABSTRACT: This work reports a versatile polymer platform that produces high molecular weight polymers containing triphenylmethane-based backbones with highly tailorable chemical structures via facile Friedel—Crafts (F—C) hydroxyalkylation polymerization and investigates their applications as gas separation membrane materials. Two series of triphenylmethane-based polymers with systematically varied substituent groups were synthesized from carefully selected monomers containing varying substituent groups. Chemical structures, thermal properties, and microstructures were comprehensively characterized. The separation performance of the polymer membranes was evaluated via conducting pure-gas permeation measurements to elucidate how substituent groups influence the fundamental gas transport properties. Variations of side



groups display dominant effects on gas diffusion processes in which bulky groups disrupt chain packing more efficiently, while steric hindrance and overall flexibility of segments also play a role, leading to diverse and highly tailorable separation performance. Some membranes in this work exhibit much-enhanced permeability and selectivity comparable to those of commercial materials. The feasible and flexible synthesis procedure as well as promising separation performance indicate the great potential of triphenylmethane-based polymers for major light—gas separations.

■ INTRODUCTION

Molecular separation processes, including gas separations, account for 10-15% of the world's energy consumption and approximately half of US industrial energy use. 1 Membranebased gas separation technology relies on the intrinsic selectivity of membrane materials instead of the intensive input energy to achieve the thermodynamic limit of demixing. Due to its low energy cost, membrane-assisted separation is promising to be combined with or replace existing thermally driven separation technologies such as cryogenic distillation, absorption, or adsorption.²⁻⁴ With the growth of gas separation membranes market (about \$1.0–1.5 billion per year^{5,6}), polymer materials (e.g., polysulfone, ^{7,8} polyimides, ⁹⁻¹⁵ polyphenylene oxide ^{16,17} and polycarbonates ¹⁸) with low cost, good processability and scalability to form membrane modules have been widely applied in industrial gas separation processes. 19,20 However, most current glassy commercial polymer materials are limited by low or moderate separation performance due to their low fractional free volume and the lack of precise control of microstructure. 21,22 Although sophisticated polymers with bulky building blocks, specifically designed functionality and/or contorted ladder-like backbones such as polymers of intrinsic microporosity (PIM) exhibit highly attractive gas separation

performance, 23-25 their complicated and expensive monomer and polymer synthesis and poor scalability hinder their practical implementation. Moreover, most glassy polymers for gas separation membranes are prepared from polycondensation reactions, which require strict 1:1 stoichiometry between the bifunctional monomers and are prone to "backbiting" and the formation of macrocycles, frequently making it difficult to readily obtain high-molecular-weight polymers.26-30 The variation of monomers' functionality could also significantly influence their reactivity in traditional polycondensation, limiting structural tunability and molecular weight. Therefore, new polymer platforms that involve feasible and flexible polymer synthesis to produce high molecular weight polymers with highly tailorable chemical structures and functionalities are highly desired to produce high performance polymer separation membrane materials.

Received: June 12, 2024 Revised: August 12, 2024 Accepted: August 13, 2024 Published: August 17, 2024





Friedel-Crafts (F-C) hydroxyalkylation polymerization between carbonyl compounds bearing electron-withdrawing groups and nonactivated aromatic hydrocarbons has been reported by Zolotukhin et al. to give linear, high-molecular-weight polymers at room temperature.^{31–34} Recently, this polymerization technique also has been used to fabricate novel fully laddered PIMs^{35,36} and biphenyl(isatin-co-trifluoroacetophenone)-based copolymers,³⁷ which exhibited high fractional free volume (FFV) and highly permeable gas transport. In our previous work, Friedel-Crafts (F-C) hydroxyalkylation reactions have been demonstrated to be a promising approach to producing high-molecular-weight and high-performance polymers without the rigorous requirement of a stoichiometric balance of monomers, metal catalysts, and/or air-sensitive procedures.³⁸ We demonstrated that a triphenylmethane-based polymer synthesized from commercially available 4-nitrobenzaldehye (NBA) and 1,4-dimethoxybenzene (DB-1) displayed ~10 times higher CO₂ permeability than commercial Matrimid polyimide while having comparable CO₂/CH₄ selectivity. Moreover, F-C hydroxyalkylation introduces a feasible way to tailor substituent groups in the macromolecular design, allowing for fine-tuning of the polymer microstructure and consequent separation performance. Specifically, triphenylmethane-based polymers obtained based on the polymerization between aryl aldehydes (BA monomers) and 1,4-disubstituted benzenes (DB monomers) (Figure 1)³⁹ have huge chemical

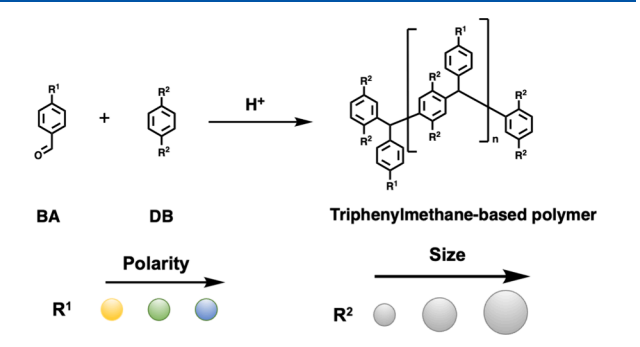


Figure 1. Triphenylmethane-based polymer design based on Friedel—Crafts (F,C) hydroxyalkylation reactions.

diversity of substituent groups (e.g., R¹ and R² on BA and DB monomers, respectively), allowing for the synthesis of a series of

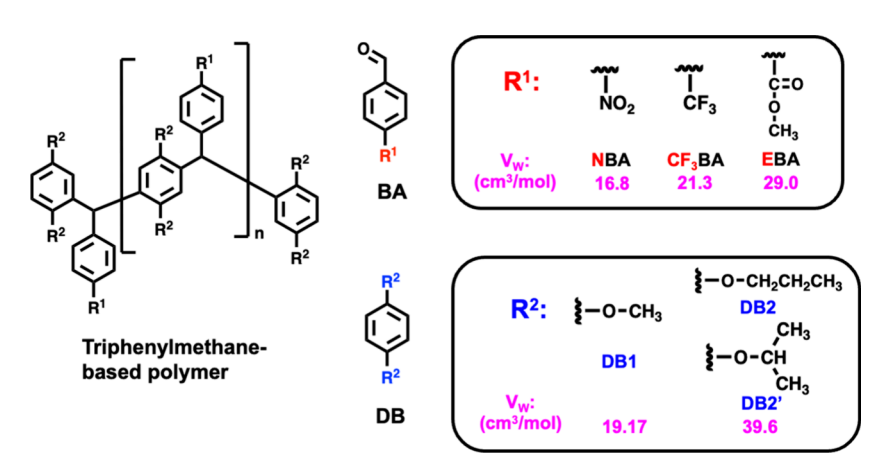
polymers with systematically varied substituent groups for fundamental structure—property relationship studies⁴⁰ to elucidate the respective effects (e.g., polarity, physical size) of substituent groups. Considering the feasibility of polymer synthesis and membrane fabrication, this work mainly focuses on elucidating how the physical size and geometric shape of substituent groups influence gas transport properties.

In this work, two distinct series of triphenylmethane-based polymers from various BA and DB monomers were produced to decouple the effects of R¹ and R² of the substituent groups on the fundamental gas transport properties. As shown in Scheme 1, polymers in the NBA series including NBA-DB1, NBA-DB2, and NBA-DB2' possess the same R1 group (i.e., -NO2) but different R² groups of varying physical size or geometrical shape. In contrast, polymers in the DB1 series, including NBA-DB1, CF₃BA-DB1, and EBA-DB1, possess the same R² group (i.e., -O-CH₃) but different R¹ groups, wherein both bulkiness and steric hindrance influence polymer chain packing. Pure-gas transport properties were studied via permeation tests for H₂, CH₄, N₂, O₂, and CO₂ at 35 °C over a wide range of feed pressures; diffusivity and solubility coefficients were calculated and analyzed to provide a fundamental understanding of gas transport properties. Based on those data, we present in-depth discussions about the synthesis, characterization, and structure property relationships of this new series of triphenylmethanebased polymers. The experimental section including materials, characterizations, synthesis of monomers and polymers, thin film preparation procedure, and gas permeation test is provided in the Supporting Information.

■ RESULTS AND DISCUSSION

Polymer Synthesis and Characterization. To investigate the effects of substituent groups, two series of polymers were designed by varying the substituents on either the electrophilic BA monomers or the nucleophilic DB monomers (Scheme 1) while keeping the other monomer standard across the series. The DB1 series consists of three polymers (i.e., NBA-DB1, CF₃BA-DB1, and EBA-DB1) with differing commercially available electrophilic BA monomers, polymerized alongside the DB1 monomer as the standard nucleophilic monomer for the series. The NBA series is composed of three polymers with differing nucleophilic DB monomers (i.e., NBA-DB1, NBA-DB2, and NBA-DB2'), which are polymerized alongside the standard electrophilic NBA monomer for the series. By setting

Scheme 1. Chemical Structures of Triphenylmethane-Based Polymers with Specifically Selected R^1 and R^2 Groups of Various van der Waals Volume (V_{wt} cm³/mol)



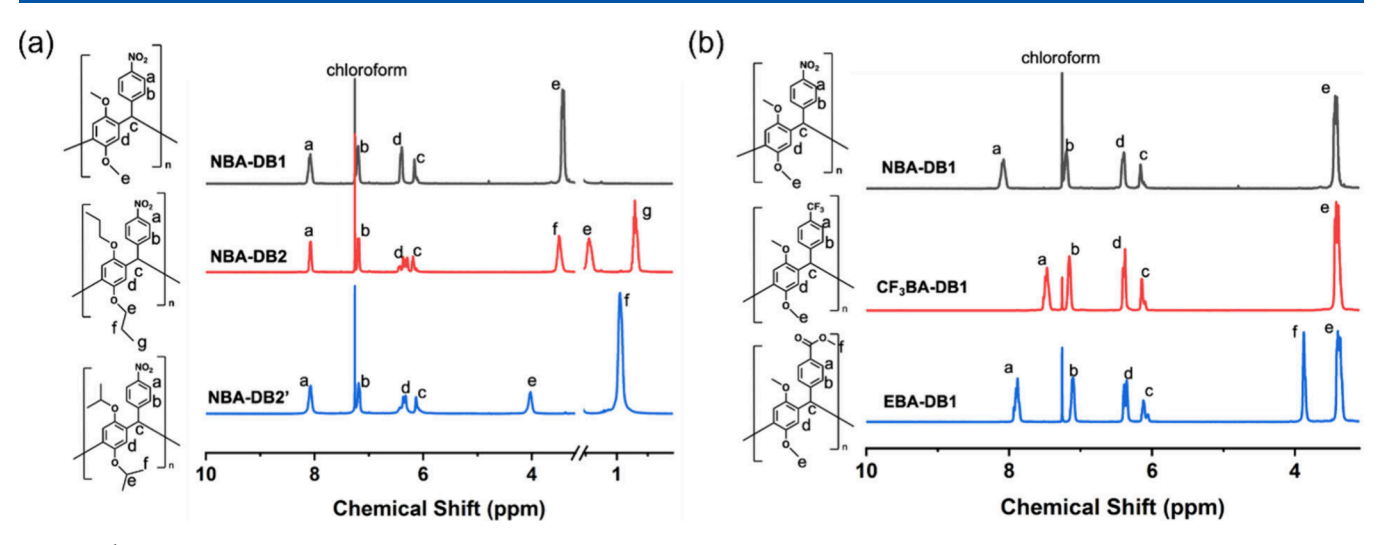


Figure 2. ¹H NMR spectra of the polymers in (a) the NBA series and (b) the DB1 series.

one monomer as the standard in each series, the effects of the varied substitution can easily be investigated. The NBA and DB1 monomers, both commercially available, were chosen as the standards for their respective series due to their high performance in the F–C polymerization and ease of achieving high molecular weights. 23

The DB2 and DB2' monomers were synthesized via the Williamson ether synthesis of hydroquinone and the respective alkyl bromide as described in the Supporting Information, with proton nuclear magnetic resonance (¹H NMR) spectra shown in Figure S1. All triarylmethane-based polymers were synthesized by dissolving in dichloromethane (DCM) before initiating polymerization with methanesulfonic acid (MSA) with feed ratios of $[DB]_0$: $[BA]_0$: $[MSA]_0 = 1:X:4$ where X = 1.1-1.3. With the exception of the EBA-DB1, all polymerizations were carried out at room temperature and $[DB]_0 = 1$ M, while the EBA-DB1 polymerization was conducted with $[DB]_0 = 2$ M. Detailed procedures can be found in the Supporting Information. ¹H NMR was employed to monitor monomer conversion through the use of 2,3-dinitro-2,3-dimethylbutane as an internal standard, with polymerization stopped once conversion of the BA monomer ceased.

Polymer structures were verified via 1H NMR spectroscopy, with each unique monomer leading to distinct shifts in the F–C backbone peaks as shown in Figure 2. All of the obtained polymers were of sufficient molecular weight to form films. Apparent number-average molar mass $(M_{\rm n})$ and polydispersity $(M_{\rm w}/M_{\rm n})$ were determined by size exclusion chromatography (SEC) based on a calibration curve of linear poly(methyl methacrylate) (PMMA) standards, with results listed in Table 1. The EBA-DB1 polymer displayed low solubility in tetrahydrofuran (THF) and was thus measured on dimethylformamide (DMF) SEC.

The thermal properties of these polymers were investigated via thermogravimetric analysis (TGA) and differential scanning calorimetry (DSC), and the results are shown in Table 1. The thermal decomposition temperatures at 5% weight loss are in the range 316–407 °C. Glass transition temperatures ($T_{\rm g}s$) of NBA-DB2 and NBA-DB2'' were not detected, while $T_{\rm g}s$ of the rest of polymers are about ~190–230 °C. Although polymer CF3BA-DB1 possesses bulky –CF3 groups ($V_{\rm w}=21.3~{\rm cm}^3/{\rm mol}$) which should largely increase the rigidity of polymer chains due to steric hindrance effects, 41,42 $T_{\rm g}$ of CF3BA-DB1 is lower than that

Table 1. Molecular Weights and Thermal Properties of Triphenylmethane-Based Polymers

Polymer ^a	$[DB]_0$: $[BA]_0$: $[MSA]_0$	Conditions	M_n^b (kg/mol)	M _w / M _n	T _{d,5%} (°C)	T _g (°C)
EBA-DB1	1:1.2:4	r.t., 24 h	201.4 ^c	1.99 ^c	407	208
CF ₃ BA- DB1	1:1.2:4	r.t., 48 h	78	2.28	395	194
NBA- DB1	1:1.2:4	r.t., 48 h	112.3	1.79	319	232
NBA- DB2	1:1.3:4	r.t., 45 h	65.6	3.22	328	-
NBA- DB2'	1:1.1:4	r.t., 96 h	38.4	3.88	316	-

"Polymer names consist of BA monomer followed by DB monomer used. ^bApparent number-average molecular weight and molecular weight distribution $(M_{\rm w}/M_{\rm n})$ measured by SEC in THF with RI detector, calibrated with linear PMMA standards. ^cApparent number-average molecular weight and molecular weight distribution $(M_{\rm w}/M_{\rm n})$ measured by SEC in DMF with RI detector, calibrated with linear PMMA standards.

of NBA-DB1 and EBA-DB1, which is likely due to its relatively lower molecular weight and broader molecular weight distribution.

Film Preparation and Characterization. Fully transparent thin films with smooth surfaces and even thickness in the range 40–70 μ m (Figure S2) were successfully fabricated following the solution casting procedures described in the Supporting Information. The densities of polymer films were measured by the buoyancy method at room temperature and were used to determine the fractional free volume (FFV) of the film based on modified Bondi's group contribution method. ⁴³ To further study polymer chain packing, densities and FFV values of thin films were compared in two series:

- (1) NBA series (NBA-DB1, NBA-DB2 and NBA-DB2'). They possess the same R^1 group (i.e., $-NO_2$) but different physical sizes or shapes of the R^2 groups ($V_{W_{DB1}} < V_{W_{DB2}} = V_{W_{NBM}}$).
- (2) <u>DB1 series (NBA-DB1, EBA-DB1 and CF₃BA-DB1)</u>. They possess the same R^2 group (i.e., $-O-CH_3$) but different R^1 groups ($V_{W_{NBA}} < V_{W_{CF3BA}} < V_{WEBA}$).

As listed in Table 2, among the three films that contain the same NBA monomer units, density decreases, while FFV

Table 2. Density, FFV, and Chain Packing Properties (WAXS) of Triphenylmethane-Based Polymer Films

	2θ			θ	d-spacing (Å)		
Samples	Film density (g/ cm³)	FFV	A	В	A	В	
EBA-DB1	1.197 ± 0.006	0.143	13.0	21.0	6.8	4.2	
CF ₃ BA- DB1	1.246 ± 0.004	0.191	13.5	19.7	6.6	4.5	
NBA-DB1	1.243 ± 0.004	0.151	12.9	21.0	6.9	4.2	
NBA-DB2	1.142 ± 0.005	0.169	9.7	20.2	9.1	4.4	
NBA-DB2'	1.135 ± 0.003	0.174	8.8	19.0	10.0	4.7	

increases with the increasing bulkiness of the R^2 groups. NBA-DB2′ displays the lowest density and, consequently, the highest FFV, which is likely related to the geometric shape of isopropoxy groups. In the DB1 series, CF_3BA -DB1 exhibits the highest FFV due to the bulkiness and steric hindrance effects of $-CF_3$. In contrast, although EBA has the largest van der Waals volume, the planar nature and flexible ether bond of the methyl ester in the EBA substituent may allow the polymer chain to pack more efficiently when compared with NBA and CF_3BA , leading to a more densely packed structure and thus the lowest FFV.

WAXS (wide-angle X-ray scattering) patterns of polymers are displayed in Figure 3, and their *d*-spacing values are tabulated in Table 2 to provide comparisons within the two series. All films exhibit two broad halos (i.e., peak A and peak B), indicating their amorphous structures. Peak A with a d-spacing value of \sim 6.6– 10.0 Å might be associated with the inefficient chain packing caused by the rigid triphenylmethane-based backbone structures, while peak B with a smaller d-spacing value of \sim 4.2–4.7 Å could be related to the interchain distance formed from the inefficient packing of less rigid segments or substituent groups. As shown in Figure 3a for NBA series, with increasing physical size of the R^2 group (i.e., DB1 < DB2 \cong DB2'), both peak A and peak B shift to smaller values, suggesting increased interchain distance typically relatable to higher fractional free volume, which is consistent with FFV results. Although the n-propoxy group (DB2) and iso-propoxy group (DB2') have the same nominal van der Waals volume, NBA-DB2' with iso-propoxy groups exhibits the largest *d*-spacing values in the NBA series, in agreement with the trend of FFV. That is likely due to the steric hindrance effects of the branched iso-propoxy group, which might more effectively frustrate chain packing and limit segmental motion leading to more loosely packed structures. In the DB1 series (Figure 3b), all three films show similar positions of peak A at about $12.9^{\circ}-13.5^{\circ}$ (*d*-spacing of \sim 6.6 – 6.9 Å) as well as similar peak B positions (*d*-spacing of \sim 4.2 – 4.5 Å). CF₃BA-DB1 displays the largest *d*-spacing value of peak B (4.5 Å), suggesting the relatively loosely packed polymer chains due to the bulky structure and steric hindrance of $-\text{CF}_3$.

Gas Transport Properties. Pure-gas permeation tests of five fresh films (NBA-DB1, NBA-DB2, NBA-DB2', EBA-DB1, and CF₃BA-DB1) were performed via a constant-volume, variable-pressure method⁴⁵ for five gases (i.e., H_2 , CH_4 , N_2 , O_2 , and CO_2) at 35 °C to elucidate how different substituent groups influence gas permeability (P) and selectivity (a) in these new triphenylmethane-based polymers. Fundamental gas transport properties, including gas diffusivity (D) and solubility (S), were also experimentally measured and calculated, respectively, to provide insight into the fundamental structure—property relationships for these polymers. Gas permeability and selectivity data, as well as diffusivity and solubility data, are listed in Table 3 for both NBA series and DB1 series. Detailed discussion on the respective effect of the R^1 (DB1 series) or R^2 (NBA series) group is as follows.

Effects of Physical Size and Geometric Shape of the R^2 *Group in NBA Series.* To investigate the effects of the R² group on the separation performance, permeability and selectivity data are compared within the NBA series, where the R² group was varied in increasing size from methoxy (DB1), n-propoxy (DB2) to iso-propoxy (DB2') while keeping the same NBA as R¹ group. As shown in Figure 4a, permeabilities of large gases (i.e., O₂, CH₄, and N₂) increase obviously with increasing the physical size of the R² group, while P_{H_2} and P_{CO_2} display relatively moderate changes. The difference suggests that large gases are more sensitive to enhanced excess free volume, which provides more pathways to allow the transport of large gas molecules. 46,47 Specifically, compared with NBA-DB1 containing methoxy groups, the CH₄ permeability of NBA-DB2 with larger npropoxy groups increases by 165%, while H2 permeability and CO₂ permeability slightly decrease by about 10–20%. Although the iso-propoxy group has the same van der Waals volume (V_w) as that of the *n*-propoxy group, NBA-DB2' exhibits the highest permeabilities for all gases in the NBA series, consistent with the results of FFV and WAXS analysis. That could be ascribed to the difference in geometric shape between n- and iso-propoxy groups. Linear n-propoxy groups are more likely to fill free volume microvoids due to their slimmer shape and flexibility, while branched iso-propoxy groups likely disrupt chain packing

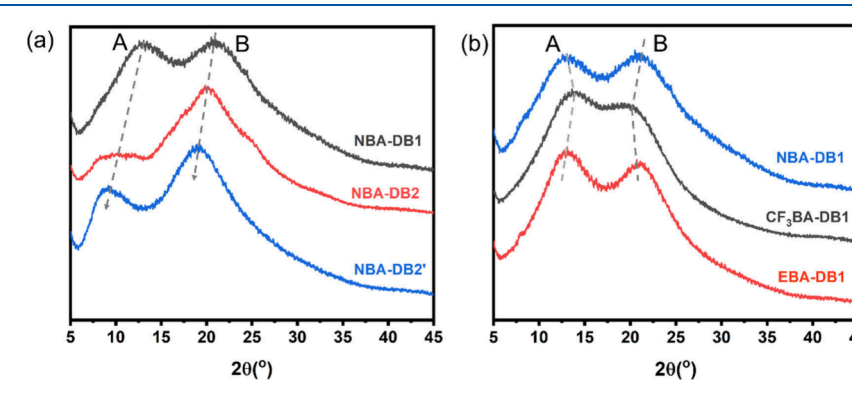


Figure 3. WAXS patterns of the (a) NBA series and (b) DB1 series.

Table 3. Pure Gas Permeability (P) (35 °C, 130 psig), Ideal Selectivity, Diffusivity Coefficient (D, 10^{-9} cm²/s), Solubility Coefficient (S, 10^{-2} cm³ (STP)/cm³ cmHg), Diffusivity Selectivity, and Solubility Selectivity of Triphenylmethane-Based Polymer Films

		Tested Gases				Ideal Selectivity				
		H_2	CO ₂	O ₂	N_2	CH ₄	H ₂ /CH ₄	O_2/N_2	CO ₂ /CH ₄	CO_2/N_2
NBA-DB1	P^a	55.3 ± 1.1	49.3 ± 1.2	6.5 ± 0.2	1.6 ± 0.04	2.0 ± 0.02	27.6 ± 1.0	4.2 ± 0.2	24.6 ± 0.9	31.8 ± 1.2
	$D^{\boldsymbol{b}}$	_	74.6 ± 3.9	125.1 ± 25.5	45.0 ± 14.5	15.8 ± 1.5	_	2.8 ± 1.1	4.7 ± 0.5	1.6 ± 0.5
	S	_	6.6 ± 0.3	0.5 ± 0.1	0.3 ± 0.1	1.3 ± 0.1	_	1.5 ± 0.6	5.2 ± 0.6	19.2 ± 6.3
NBA-DB2	P	42.4 ± 0.8	44.4 ± 1.1	9.2 ± 0.2	2.5 ± 0.1	5.3 ± 0.1	8.0 ± 0.2	3.6 ± 0.1	8.4 ± 0.3	17.4 ± 0.6
	D	_	145.0 ± 7.8	333.4 ± 116.4	112.7 ± 46.6	83.6 ± 12.7	_	3.0 ± 1.6	1.7 ± 0.3	1.3 ± 0.5
	S	-	3.1 ± 0.2	0.3 ± 0.1	0.2 ± 0.1	0.6 ± 0.1	_	1.2 ± 0.1	4.8 ± 0.8	13.5 ± 5.7
NBA-DB2'	P	79.3 ± 1.3	74.3 ± 1.6	15.6 ± 0.3	4.0 ± 0.1	7.1 ± 0.2	11.1 ± 0.3	3.9 ± 0.1	10.4 ± 0.3	18.7 ± 0.6
	D	_	157.9 ± 2.9	423.9 ± 76.9	158.1 ± 40.4	73.3 ± 5.1	_	2.7 ± 0.8	2.2 ± 0.2	1.0 ± 0.2
	S	_	5.2 ± 0.1	0.4 ± 0.1	0.3 ± 0.1	1.0 ± 0.1	_	1.5 ± 0.5	5.2 ± 0.5	20.7 ± 5.4
EBA-DB1	P	42.9 ± 0.8	32.0 ± 0.6	5.4 ± 0.1	1.3 ± 0.02	1.4 ± 0.03	29.8 ± 0.8	4.3 ± 0.1	22.2 ± 0.6	25.3 ± 0.7
	D	_	58.2 ± 1.3	101.9 ± 24.3	41.2 ± 15.4	11.9 ± 1.1	_	2.5 ± 1.1	4.9 ± 0.5	1.4 ± 0.5
	S	_	6.0 ± 0.2	0.5 ± 0.1	0.3 ± 0.1	1.2 ± 0.1	_	1.7 ± 0.7	4.9 ± 0.5	19.2 ± 7.2
CF ₃ BA-	P	223 ± 4.3	293.0 ± 3.1	57.1 ± 1.1	17.8 ± 0.3	23.2 ± 0.4	9.6 ± 0.3	3.2 ± 0.1	12.6 ± 0.3	16.4 ± 0.4
DB1	D	_	603.5 ± 63.2	939.2 ± 110.5	736.4 ± 214.2	441.3 ± 59.5	_	1.3 ± 0.4	1.8 ± 0.2	0.8 ± 0.3
	S	_	3.8 ± 0.6	0.6 ± 0.1	0.2 ± 0.1	0.5 ± 0.1	_	2.5 ± 0.8	7.8 ± 1.8	23.0 ± 7.2

 a Units: P, 1 Barrer = 10^{-10} cm 3 (STP)*cm/cm 2 *s*cmHg; D, 10^{-9} cm 2 /s; S, 10^{-2} cm 3 (STP)/cm 3 *cmHg. b H $_2$ diffusivity coefficients were not determined due to the very short lag time. All diffusivity coefficients were calculated from the lag time and the pure gas permeability at 30 psig.

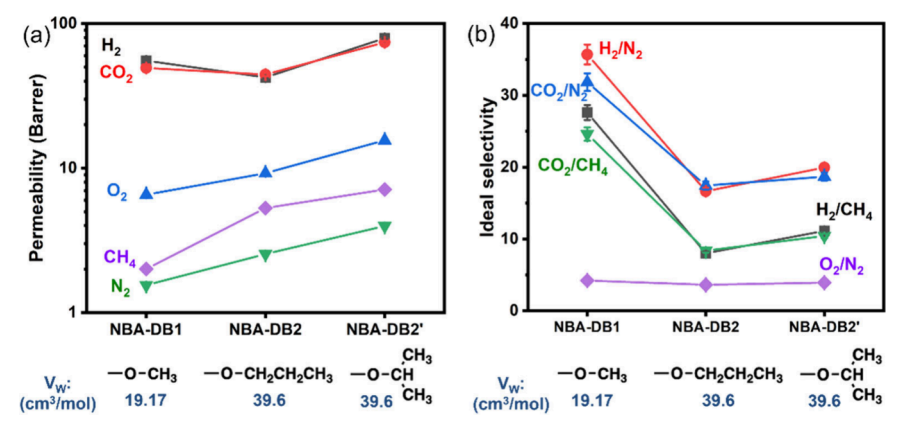


Figure 4. (a) Pure-gas permeability and (b) ideal selectivity of the NBA series (NBA-DB1, NBA-DB2, and NBA-DB2') with various R^2 groups differing in physical size (indicated by V_w values underneath the structure of the R^2 groups) at 35 °C, 130 psig.

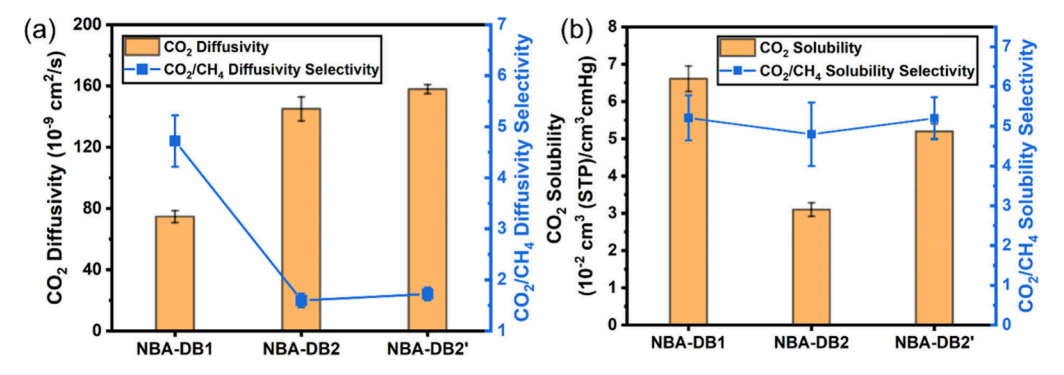


Figure 5. (a) CO_2 diffusivity and CO_2/CH_4 diffusivity selectivity of the NBA series. (b) CO_2 solubility and CO_2/CH_4 solubility selectivity of the NBA series.

more efficiently, resulting in the most loosely packed structures in the NBA series.

The physical size and geometric shape of the R² group also display a significant influence on the size-sieving property of the

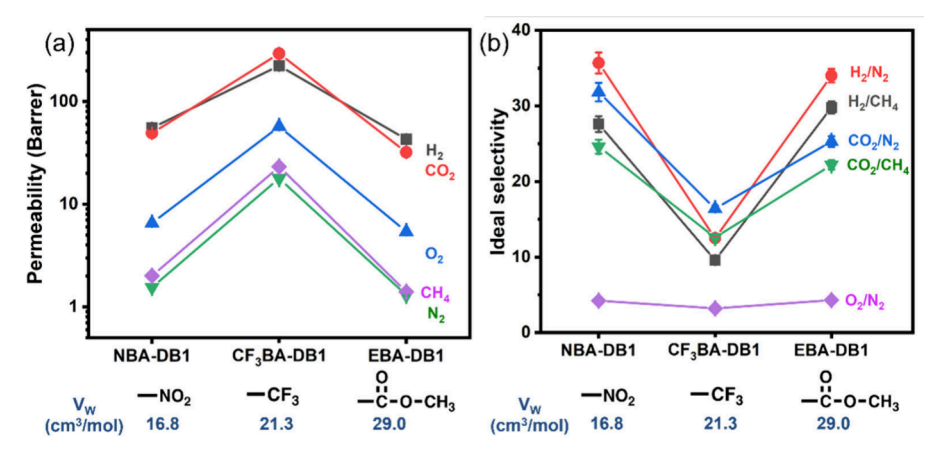


Figure 6. (a) Permeability and (b) ideal selectivity of the DB1 series (NBA-DB1, $CF_3BA-DB1$, and EBA-DB1) with various R^1 groups differing in physical size (indicated by V_W values underneath the structure of the R^1 groups) at 35 °C and 130 psig.

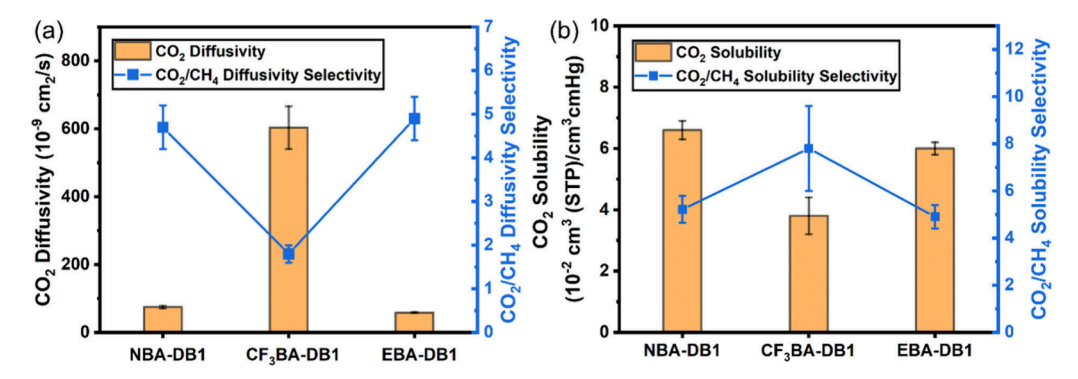


Figure 7. (a) CO₂ diffusivity and CO₂/CH₄ diffusivity selectivity of the DB1 series. (b) CO₂ solubility and CO₂/CH₄ solubility selectivity of the DB1 series

NBA series. With increasing physical size, ideal selectivity (α) values largely decline for most gas pairs (Figure 4b). Compared with NBA-DB1, the $\rm H_2/CH_4$ selectivity of NBA-DB2 decreases by 71%, and the $\rm O_2/N_2$ selectivity also decreases by 14%. The impaired size-sieving ability is also likely due to more open microstructures with the incorporation of bulkier n-propoxy groups. Compared with NBA-DB2, the iso-propoxy containing NBA-DB2' exhibits comparable or slightly higher ideal selectivity for all gas pairs, which are further elucidated via the analysis of diffusivity selectivity and solubility selectivity in the following paragraphs.

Diffusivity coefficients (D) were determined via the time-lag method, and solubility coefficients (S) were then calculated according to the solution-diffusion model.⁴⁸ Correspondingly, diffusivity selectivity and solubility selectivity were calculated, and all of the results are listed in Table 3. As shown in Figure 5a using the CO₂/CH₄ gas pair as an example, with increasing physical size of the R² group, both NBA-DB2 and NBA-DB2' exhibit much higher gas diffusivities than NBA-DB1, consistent with the trend of permeability as a function of the R² group. An increase in the size of the R² group leads to declined CO₂/CH₄ diffusivity selectivity as expected (e.g., ~47% decrease in NBA-DB2 and ~53% decrease in NBA-DB2' relative to NBA-DB1), suggesting the impaired size-sieving ability with large substituent groups. Between NBA-DB2 and NBA-DB2', the effect of geometric shape does not seem to be of significance on diffusivity selectivity, particularly when errors are included. On the other hand, the trend of solubility coefficients is less straightforward (Figure 5b). Unlike the trend of CO₂ diffusivity coefficients, CO_2 solubility coefficients display much less significant changes with the variation of R^2 groups, indicating the dominant role of diffusion process in these polymers. Considering the uncertainties of the time-lag method, solubility selectivity does not change a lot within the NBA series. Therefore, with the increasing physical size of the R^2 group, the declined ideal selectivity could be mainly ascribed to a greatly reduced diffusivity selectivity.

Effects of Physical Size and Steric Hindrance of the R¹ *Group.* To investigate the effects of the R¹ group on separation performance, permeability and selectivity data are compared within the DB1 series, where different R1 groups including -NO₂ (NBA-DB1), -CF₃ (CF₃BA-DB1) and -COOCH₃ (EBA-DB1) were incorporated while keeping the same methoxy group (DB1) as the R² group. According to Figure 6a, permeability coefficients of DB1 series films show a nonmonotonic trend with increasing van der Waals volume of the R¹ group $(V_{W_{-NO2}} < V_{W_{-CF3}} < V_{W_{-COOCH3}})$. CF₃BA-DB1 displays significantly higher permeability (e.g., ~300% higher H₂ permeability relative to NBA-DB1 and ~960% higher O2 permeability relative to EBA-DB1), likely due to the geometric feature of R¹ groups. Specifically, the three bulky fluorine atoms in the -CF₃ group effectively impose strong steric hindrance effects that can limit mobility or free rotation of chain segments, resulting in a loosely packed structure leading to high permeability. 49,50 Additionally, despite its largest van der Waals volume among the R1 groups, the planar nature of the -COOCH₃ substituent likely leads to more densely packed segments and thus exhibits even lower permeability than NBA-

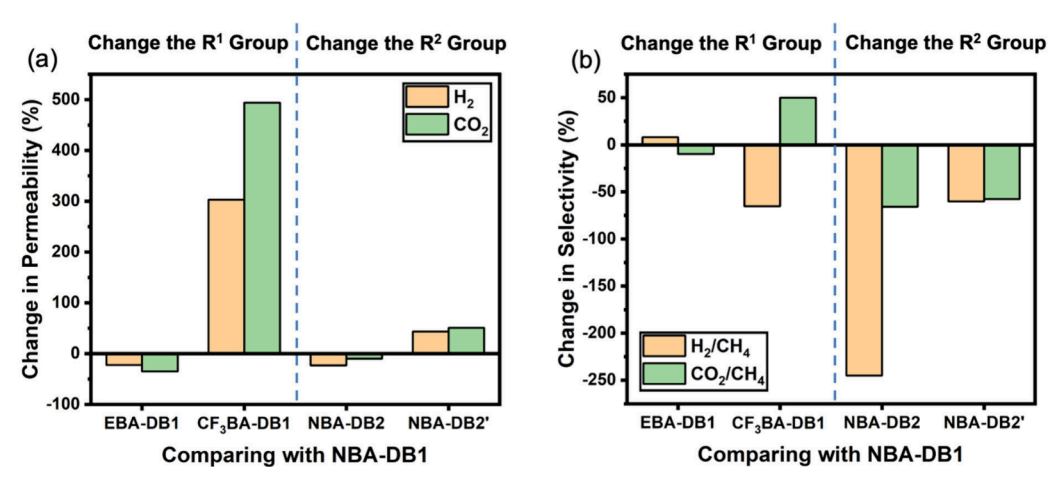


Figure 8. Percentage changes in (a) permeability and (b) selectivity of films relative to the NBA-DB1 due to the change of the R¹ group or the R² group.

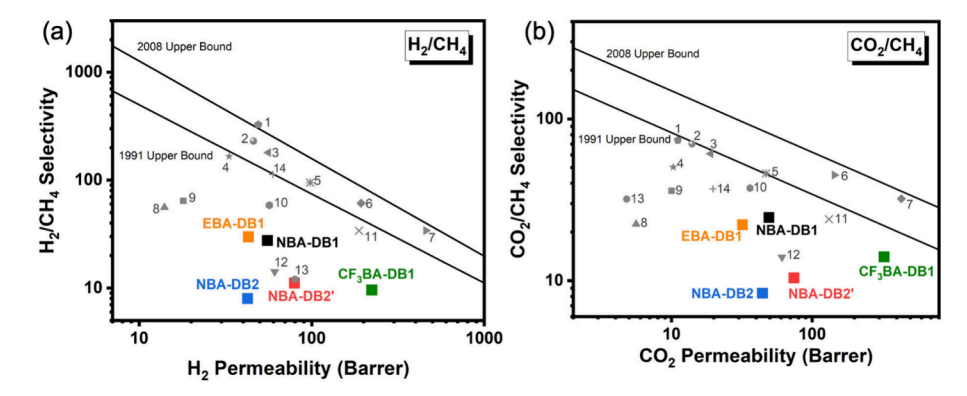


Figure 9. Gas separation performance of triphenylmethane-based polymer films for (a) H_2/CH_4 and (b) CO_2/CH_4 . Commercial polymer films and high-performance polyimide-based membranes are included for comparison. Polymers are labeled as follows: (1) 6FDA-DABA; (2) 6FDA-mPDA; (3) 6FDA-TrMSA; (4) ODA/DABA (7:3); (5) CF_3 : (5) CF_3 : (6) 6FDA-TrMCA; (7) FDDA; (8) PSF; (9) Matrimid; (10) ODA/APAF (7:3); (11) 6FDA-PPDA (CF₃); (12) PPO; (13) CA-2.45; (14) 6FDA-1,4-trip (CF₃).

DB1 with the smallest $-NO_2$ substitution. Correspondingly, ideal selectivity for several gas pairs exhibits a nonmonotonic trend, where CF_3BA -DB1 displays the lowest selectivity values following the typical permeability-selectivity trade-off relationship (Figure 6b).

Diffusivity (D) and solubility (S) coefficients of DB1 series films, as well as corresponding diffusivity selectivity ($D_{\rm A}/D_{\rm B}$) and solubility ($S_{\rm A}/S_{\rm B}$) selectivity, were measured or calculated as listed in Table 3. The dependence of diffusivity on the R¹ group shows the same trend as that of the permeability (Figure 7a). With the presence of $-CF_3$ groups, $CF_3BA-DB1$ exhibits the highest diffusivities for all gases among the DB1 series, while EBA-DB1 containing the largest but more planar -COOMe groups shows the lowest diffusivity coefficients in this series. This trend also indicates that steric hindrance of substituent groups and flexibility of segments could influence polymer chain packing more significantly than the physical size. The dependence of diffusivity selectivity on the R¹ group shows an expected trade-off trend, where polymers with high diffusivities tend to have low diffusivity selectivity.

Solubility coefficients seem to be less sensitive to the variation of the R^1 group (Figure 7b). With the variation of the R^1 group, all three membranes in the DB1 series display similar solubility coefficients, suggesting that diffusion dominates gas transport in these new triphenylmethane-based polymers. As shown in Table 3, $CF_3BA-DB1$ displays slightly higher CO_2/CH_4 solubility selectivity values than the other two polymers in the DB1 series,

which might be related to the high affinity of CF₃ groups with CO₂ molecules. However, the enhanced solubility selectivity could not offset the largely decreased diffusivity selectivity, leading to the lowest overall ideal selectivity of CF₃BA-DB1 among the DB1 series.

Overall Gas Separation Performance. CO_2 plasticization behavior of all membranes was studied via plotting CO_2 permeability versus upstream pressure (i.e., 30-230 psi) in Figure S3. With increasing upstream pressure, CO_2 permeability slightly decreases which corresponds with the typical behavior of glassy polymers according to the dual-mode sorption model. S3,S4 The plasticization point could not be detected within the testing range, suggesting the attractive resistance to CO_2 plasticization due to the rigid triphenylmethane polymer backbone.

While multiple variables between the BA and DB series were adjusted, including polarity, size, and number of substituents per repeating unit, a cursory comparison between the series illustrates the effect on substituent position for tailoring gas transport properties. The changes in permeabilities and selectivities by adjusting the R^1 or the R^2 groups are compared in Figure 8. It seems that varying the R^1 group could tailor gas permeabilities more efficiently while better maintaining the size-sieving capability than systematically adjusting the R_2 groups. Bulky groups with large steric hindrances (i.e., $-CF_3$ groups) play an important role in disrupting chain packing and improving gas permeabilities. In contrast, the H_2/CH_4 and CO_2/CH_4 selectivities are more sensitive to variation of the R^2

group. Compared with *n*-propoxy (DB2) and iso-propoxy (DB2'), the methoxy group (DB1) seems to contribute to the well-maintained size-sieving capability, resulting in the overall more promising selectivities of the DB1 series.

To evaluate the overall separation performance of triphenylmethane-based polymers, permeability and selectivity data are plotted together with the Robeson upper bound in Figure 9 and Figure S4. Data of some commercial polymer films, e.g., Matrimid polyimide, cellulose acetate with 2.45 deg of acetylation (CA-2.45), polysulfone (PSF) and poly(2,6dimethylpheylene oxide) (PPO), as well as high-performance polyimide-based membranes reported in recent years, are also included for comparison. Overall separation performance of EBA-DB1, NBA-DB1, and CF₃BA-DB1 is comparable to or even outperforms those commercial materials, judging by the distance between the data points and the upper bound. Additionally, the highly diverse chemical structures of triphenylmethane-based polymers make it feasible to finely tailor the separation performance by incorporating diverse substituent groups. With bulky -CF₃ groups, the newly synthesized CF₃BA-DB1 exhibits a largely improved permeability without significant sacrifice of selectivity. The H2 permeability and CO2 permeability of CF₃BA-DB1 were more than 9 and 14 times higher than those of Matrimid, respectively. By incorporating planar -COOMe or small -NO2 groups, the size-sieving property is largely improved, resulting in \sim 100% higher H_2/CH_4 selectivity and ~47% higher CO₂/CH₄ selectivity than PPO.

CONCLUSIONS

Two series of novel triphenylmethane-based polymers with various substituent groups have been successfully synthesized via facile F-C polycondensation from a series of BA and DB monomers with specifically chosen substituent groups for systematic structure-property relationship studies. Obtained high-molecular-weight polymers could be readily cast into freestanding thin films, of which their gas separation performances were comprehensively evaluated at ambient conditions with five light gases. Through independent investigation on the two series of polymers with varied substituent groups as well as systematic comparisons between the two series of polymers, we were able to decouple the effects of R¹ and R² groups. Bulky R² groups on DB monomers (i.e., propoxy) are able to effectively improve permeability and diffusivity coefficients of gases by disrupting chain packing, while the small methoxy group seems to make a significant contribution to the size-sieving capability. The steric hindrance of R1 groups on the BA series plays an important role in limiting segmental motion and thus improving permeability. With highly tailorable chemical structures, triphenylmethane-based polymers display a wide range of gas separation performance that can be finely tailored by incorporating different R1 and R2 groups to meet various gas separation needs. The permeability can be effectively tailored by varying the bulkiness and steric hindrance properties of the R¹ group, while the selectivity can be optimized when the methoxy group is used as the R² group. As a result, all newly synthesized thin films realize a much-enhanced permeability and comparable selectivity with commercial polymer materials. The easily available monomer sources and facile synthesis procedure also indicate the great potential of this new polymer platform for applications of gas separations.

ASSOCIATED CONTENT

Solution Supporting Information

The Supporting Information is available free of charge at https://pubs.acs.org/doi/10.1021/acs.macromol.4c01361.

The experimental section including materials, characterizations, synthesis of monomers and polymers, thin film preparation procedure, and gas separation measurements can be found in the Supporting Information. (PDF)

AUTHOR INFORMATION

Corresponding Authors

Ruilan Guo — Department of Chemical and Biomolecular Engineering, University of Notre Dame, Notre Dame, Indiana 46S56, United States; orcid.org/0000-0002-3373-2588; Email: rguo@nd.edu

Haifeng Gao – Department of Chemistry and Biochemistry, University of Notre Dame, Notre Dame, Indiana 46556, United States; ⊚ orcid.org/0000-0001-9029-5022; Email: gaohaifeng1@gmail.com

Authors

Mengdi Liu — Department of Chemical and Biomolecular Engineering, University of Notre Dame, Notre Dame, Indiana 46556, United States; orcid.org/0000-0002-8571-3450

Andrew Trowbridge — Department of Chemistry and Biochemistry, University of Notre Dame, Notre Dame, Indiana 46556, United States; Oorcid.org/0009-0007-1438-2862

Alexander Hymes — Department of Chemistry and Biochemistry, University of Notre Dame, Notre Dame, Indiana 46556, United States

Complete contact information is available at: https://pubs.acs.org/10.1021/acs.macromol.4c01361

Author Contributions

§M.L. and A.T. contributed equally to this work.

Notes

The authors declare no competing financial interest.

ACKNOWLEDGMENTS

The authors are thankful for the financial support from the National Science Foundation (CBET-2006242) and the University of Notre Dame. A.T. and H.G. also are thankful for the financial support from the ACS Petroleum Research Fund (PRF #59601-ND7).

■ REFERENCES

- (1) Sholl, D. S.; Lively, R. P. Seven chemical separations to change the world. *Nature* **2016**, *532* (7600), 435–437.
- (2) Castel, C.; Favre, E. Membrane separations and energy efficiency. *J. Membr. Sci.* **2018**, 548, 345–357.
- (3) Koros, W. J.; Lively, R. P. Water and beyond: Expanding the spectrum of large-scale energy efficient separation processes. *AIChE J.* **2012**, 58 (9), 2624–2633.
- (4) Yang, L.; Qian, S.; Wang, X.; Cui, X.; Chen, B.; Xing, H. Energy-efficient separation alternatives: metal—organic frameworks and membranes for hydrocarbon separation. *Chem. Soc. Rev.* **2020**, 49 (15), 5359–5406.
- (5) Galizia, M.; Chi, W. S.; Smith, Z. P.; Merkel, T. C.; Baker, R. W.; Freeman, B. D. 50th anniversary perspective: polymers and mixed matrix membranes for gas and vapor separation: a review and prospective opportunities. *Macromolecules* **2017**, *50* (20), 7809–7843.
- (6) Ulbricht, M. Advanced functional polymer membranes. *Polymer* **2006**, 47 (7), 2217–2262.

- (7) McHattie, J. S.; Koros, W. J.; Paul, D. R. Gas transport properties of polysulphones: 3. Comparison of tetramethyl-substituted bisphenols. *Polymer* **1992**, 33 (8), 1701–1711.
- (8) Aitken, C. L.; Koros, W. J.; Paul, D. R. Effect of structural symmetry on gas transport properties of polysulfones. *Macromolecules* **1992**, 25 (13), 3424–3434.
- (9) Ekiner, O. M.; Vassilatos, G. Polyaramide hollow fibers for $\rm H_2/$ CH₄ separation: II. Spinning and properties. *J. Membr. Sci.* **2001**, 186 (1), 71–84.
- (10) Bos, A.; Pünt, I. G. M.; Wessling, M.; Strathmann, H. Plasticization-resistant glassy polyimide membranes for CO_2/CO_4 separations. *Sep. Purif. Technol.* **1998**, *14* (1), 27–39.
- (11) Sanaeepur, H.; Ebadi Amooghin, A.; Bandehali, S.; Moghadassi, A.; Matsuura, T.; Van der Bruggen, B. Polyimides in membrane gas separation: Monomer's molecular design and structural engineering. *Prog. Polym. Sci.* **2019**, *91*, 80–125.
- (12) Wind, J. D.; Paul, D. R.; Koros, W. J. Natural gas permeation in polyimide membranes. J. Membr. Sci. 2004, 228 (2), 227–236.
- (13) Xiao, Y.; Low, B. T.; Hosseini, S. S.; Chung, T. S.; Paul, D. R. The strategies of molecular architecture and modification of polyimide-based membranes for CO₂ removal from natural gas—A review. *Prog. Polym. Sci.* **2009**, *34* (6), 561–580.
- (14) Xu, Z.; Croft, Z. L.; Guo, D.; Cao, K.; Liu, G. Recent development of polyimides: Synthesis, processing, and application in gas separation. *J. Polym. Sci.* **2021**, *59* (11), 943–962.
- (15) Wang, R.; Cao, C.; Chung, T.-S. A critical review on diffusivity and the characterization of diffusivity of 6FDA-6FpDA polyimide membranes for gas separation. *J. Membr. Sci.* **2002**, *198* (2), 259–271.
- (16) Percec, S.; Li, G. Chemical Modification of Poly(2,6-dimethyl-1,4-phenylene oxide) and Properties of the Resulting Polymers. In *Chemical Reactions on Polymers*, ACS Symposium Series, Vol. 364; American Chemical Society: 1988; pp 46–59.
- (17) Story, B. J.; Koros, W. J. Sorption and transport of CO_2 and CH_4 in chemically modified poly(phenylene oxide). *J. Membr. Sci.* **1992**, 67 (2), 191–210.
- (18) Muruganandam, N.; Koros, W.; Paul, D. Gas sorption and transport in substituted polycarbonates. *J. Polym. Sci., Part B: Polym. Phys.* **1987**, 25 (9), 1999–2026.
- (19) Sanders, D. F.; Smith, Z. P.; Guo, R.; Robeson, L. M.; McGrath, J. E.; Paul, D. R.; Freeman, B. D. Energy-efficient polymeric gas separation membranes for a sustainable future: A review. *Polymer* **2013**, *54* (18), 4729–4761.
- (20) Scott, K.; Hughes, R.; Hughes, R. *Industrial membrane separation technology*; Springer Science & Business Media: 1996.
- (21) Freeman, B. D. Basis of Permeability/Selectivity Tradeoff Relations in Polymeric Gas Separation Membranes. *Macromolecules* 1999, 32 (2), 375–380.
- (22) Tin, P. S.; Chung, T. S.; Liu, Y.; Wang, R.; Liu, S. L.; Pramoda, K. P. Effects of cross-linking modification on gas separation performance of Matrimid membranes. *J. Membr. Sci.* **2003**, 225 (1), 77–90.
- (23) Budd, P. M.; Msayib, K. J.; Tattershall, C. E.; Ghanem, B. S.; Reynolds, K. J.; McKeown, N. B.; Fritsch, D. Gas separation membranes from polymers of intrinsic microporosity. *J. Membr. Sci.* **2005**, 251 (1), 263–269.
- (24) McKeown, N. B.; Budd, P. M. Polymers of intrinsic microporosity (PIMs): organic materials for membrane separations, heterogeneous catalysis and hydrogen storage. *Chem. Soc. Rev.* **2006**, 35 (8), 675–683.
- (25) McKeown, N. B.; Budd, P. M. Exploitation of intrinsic microporosity in polymer-based materials. *Macromolecules* **2010**, 43 (12), 5163–5176.
- (26) Stille, J. K. Step-growth polymerization; ACS Publications: 1981.
- (27) Odian, G. Principles of polymerization; John Wiley & Sons: 2004.
- (28) Kricheldorf, H. R. Macrocycles. 21. Role of Ring—Ring Equilibria in Thermodynamically Controlled Polycondensations. *Macromolecules* **2003**, 36 (7), 2302–2308.
- (29) Kricheldorf, H. R.; Weidner, S. M.; Scheliga, F. Synthesis of cyclic polymers and flaws of the Jacobson—Stockmayer theory. *Polym. Chem.* **2020**, *11* (14), 2595–2604.

- (30) Kricheldorf, H. R. Cyclic and Multicyclic Polymers by Three-Dimensional Polycondensation. *Acc. Chem. Res.* **2009**, 42 (8), 981–992
- (31) Zolotukhin, M.; Fomine, S.; Salcedo, R.; Khalilov, L. Remarkable enhancement of reactivity of carbonyl compounds for polymerizations with non-activated aromatic hydrocarbons. *Chem. Commun.* **2004**, No. 8, 1030–1031.
- (32) Zolotukhin, M. G.; Fomina, L.; Salcedo, R.; Sansores, L. E.; Colquhoun, H. M.; Khalilov, L. M. Superelectrophiles in Polymer Chemistry. A Novel, One-Pot Synthesis of High-T g, High-Temperature Polymers. *Macromolecules* **2004**, 37 (14), 5140–5141.
- (33) Zolotukhin, M. G.; Fomine, S.; Lazo, L. M.; Salcedo, R.; Sansores, L. E.; Cedillo, G. G.; Colquhoun, H. M.; Fernandez-G, J. M.; Khalizov, A. F. Superacid-Catalyzed Polycondensation of Acenaphthenequinone with Aromatic Hydrocarbons. *Macromolecules* **2005**, 38 (14), 6005–6014.
- (34) Hernandez, M. C. G.; Zolotukhin, M. G.; Fomine, S.; Cedillo, G.; Morales, S. L.; Fröhlich, N.; Preis, E.; Scherf, U.; Salmón, M.; Chávez, M. I.; Cárdenas, J.; Ruiz-Trevino, A. Novel, Metal-Free, Superacid-Catalyzed "Click" Reactions of Isatins with Linear, Nonactivated, Multiring Aromatic Hydrocarbons. *Macromolecules* **2010**, *43* (17), 6968–6979.
- (35) Cai, Z.; Liu, Y.; Wang, C.; Xie, W.; Jiao, Y.; Shan, L.; Gao, P.; Wang, H.; Luo, S. Ladder polymers of intrinsic microporosity from superacid-catalyzed Friedel-Crafts polymerization for membrane gas separation. *J. Membr. Sci.* 2022, 644, No. 120115.
- (36) Zhu, Z.; Dong, H.; Li, K.; Li, Q.; Li, J.; Ma, X. One-step synthesis of hydroxyl-functionalized fully carbon main chain PIMs via a Friedel-Crafts reaction for efficient gas separation. *Sep. Purif. Technol.* **2021**, 262, No. 118313.
- (37) Hossain, I.; Husna, A.; Jeong, I.; Kim, T.-H. Biphenyl(isatin-cotrifluoroacetophenone)-Based Copolymers Synthesized Using the Friedel—Crafts Reaction as Mechanically Robust Membranes for Efficient CO₂ Separation. ACS Applied Polymer Materials **2022**, 4 (5), 3779—3790.
- (38) Zou, L.; Cao, X.; Zhang, Q.; Dodds, M.; Guo, R.; Gao, H. Friedel—Crafts A2 + B4 Polycondensation toward Regioselective Linear Polymer with Rigid Triphenylmethane Backbone and Its Property as Gas Separation Membrane. *Macromolecules* **2018**, *51* (17), 6580—6586.
- (39) Gao, H. Synthesis of Linear Polymers in High Molecular Weights via Reaction-Enhanced Reactivity of Intermediates Using Friedel—Crafts Polycondensation. *ACS omega* **2021**, *6* (7), 4527–4533.
- (40) Cuneo, T.; Cao, X.; Zou, L.; Gao, H. Synthesis of multisegmented block copolymer by Friedel–Crafts hydroxyalkylation polymerization. *Polym. Chem.* **2020**, *11* (14), 2542–2549.
- (41) Luo, S.; Liu, Q.; Zhang, B.; Wiegand, J. R.; Freeman, B. D.; Guo, R. Pentiptycene-based polyimides with hierarchically controlled molecular cavity architecture for efficient membrane gas separation. *J. Membr. Sci.* **2015**, *480*, 20–30.
- (42) Wiegand, J. R.; Smith, Z. P.; Liu, Q.; Patterson, C. T.; Freeman, B. D.; Guo, R. Synthesis and characterization of triptycene-based polyimides with tunable high fractional free volume for gas separation membranes. *Journal of Materials Chemistry A* **2014**, 2 (33), 13309–13320.
- (43) Park, J. Y.; Paul, D. R. Correlation and prediction of gas permeability in glassy polymer membrane materials via a modified free volume based group contribution method. *J. Membr. Sci.* **1997**, *125* (1), 23–39.
- (44) Wang, S.; Jin, S.; Han, X.; Li, L.; Zhao, X.; Zhou, H.; Chen, C. Insights into the relationship between structure and properties of Spirobichroman-based polyimides: Effects of substituents on molecular structure and gas separation. *Materials & Design* **2020**, 194, No. 108933.
- (45) Pye, D.; Hoehn, H.; Panar, M. Measurement of gas permeability of polymers. I. Permeabilities in constant volume/variable pressure apparatus. J. Appl. Polym. Sci. 1976, 20 (7), 1921–1931.

- (46) Low, Z.-X.; Budd, P. M.; McKeown, N. B.; Patterson, D. A. Gas permeation properties, physical aging, and its mitigation in high free volume glassy polymers. *Chem. Rev.* **2018**, *118* (12), 5871–5911.
- (47) Maeda, Y.; Paul, D. Effect of antiplasticization on gas sorption and transport. III. Free volume interpretation. *J. Polym. Sci., Part B: Polym. Phys.* **1987**, 25 (5), 1005–1016.
- (48) Wijmans, J. G.; Baker, R. W. The solution-diffusion model: a review. *Journal of membrane science* **1995**, 107(1-2), 1-21.
- (49) Finkelshtein, E. S.; Bermeshev, M. V.; Gringolts, M. L.; Starannikova, L.; Yampolskii, Y. P. Substituted polynorbornenes as promising materials for gas separation membranes. *Russ. Chem. Rev.* **2011**, *80* (4), 341.
- (50) Bermeshev, M.; Starannikova, L.; Sterlin, S.; Tyutyunov, A.; Tavtorkin, A.; Yampolskii, Y. P.; Finkelshtein, E. S. Synthesis and gasseparation properties of metathesis poly (3-fluoro-3-pentafluoroethyl-4, 4-bis (trifluoromethyl) tricyclonene-7). *Petroleum Chemistry* **2015**, 55 (9), 753–758.
- (51) Wu, D.; Yi, C.; Doherty, C. M.; Lin, L.; Xie, Z. A Crown Ether-Containing Copolyimide Membrane with Improved Free Volume for CO₂ Separation. *Ind. Eng. Chem. Res.* **2019**, 58 (31), 14357–14367.
- (52) Lin, Y. F.; Chen, C. H.; Tung, K. L.; Wei, T. Y.; Lu, S. Y.; Chang, K. S. Mesoporous Fluorocarbon-Modified Silica Aerogel Membranes Enabling Long-Term Continuous CO₂ Capture with Large Absorption Flux Enhancements. *ChemSusChem* **2013**, *6* (3), 437–442.
- (53) Vieth, W. R.; Howell, J.; Hsieh, J. Dual sorption theory. *J. Membr. Sci.* **1976**, *I* (2), 177–220.
- (54) Kanehashi, S.; Nagai, K. Analysis of dual-mode model parameters for gas sorption in glassy polymers. *J. Membr. Sci.* **2005**, 253 (1–2), 117–138.
- (55) Ma, X.; Mukaddam, M.; Pinnau, I. Bifunctionalized Intrinsically Microporous Polyimides with Simultaneously Enhanced Gas Permeability and Selectivity. *Macromol. Rapid Commun.* **2016**, *37* (11), 900–904.
- (56) Alaslai, N.; Ghanem, B.; Alghunaimi, F.; Litwiller, E.; Pinnau, I. Pure- and mixed-gas permeation properties of highly selective and plasticization resistant hydroxyl-diamine-based 6FDA polyimides for CO₂/CH₄ separation. *J. Membr. Sci.* **2016**, 505, 100–107.
- (57) Abdulhamid, M. A.; Genduso, G.; Ma, X.; Pinnau, I. Synthesis and characterization of 6FDA/3,5-diamino-2,4,6-trimethylbenzenesulfonic acid-derived polyimide for gas separation applications. *Sep. Purif. Technol.* **2021**, 257, No. 117910.
- (58) Jia, P.; Liu, J.; Kong, J.; Hu, M.; Qi, N.; Chen, Z.; Xu, S.; Li, N. Tailoring the micropore structure of 6FDA-based polyimide membrane for gas permselectivity studied by positron annihilation. *Sep. Purif. Technol.* **2022**, 282, No. 120044.
- (59) Weidman, J. R.; Luo, S.; Breier, J. M.; Buckley, P.; Gao, P.; Guo, R. Triptycene-based copolyimides with tailored backbone rigidity for enhanced gas transport. *Polymer* **2017**, *126*, 314–323.
- (60) Abdulhamid, M. A.; Genduso, G.; Wang, Y.; Ma, X.; Pinnau, I. Plasticization-Resistant Carboxyl-Functionalized 6FDA-Polyimide of Intrinsic Microporosity (PIM–PI) for Membrane-Based Gas Separation. *Ind. Eng. Chem. Res.* **2020**, *59* (12), 5247–5256.
- (61) Wu, D.; Zhang, B.; Yuan, J.; Yi, C. Structural engineering on 6FDA-Durene based polyimide membranes for highly selective gas separation. *Sep. Purif. Technol.* **2023**, *316*, No. 123786.
- (62) Huang, Y.; Paul, D. R. Effect of Film Thickness on the Gas-Permeation Characteristics of Glassy Polymer Membranes. *Ind. Eng. Chem. Res.* **2007**, 46 (8), 2342–2347.
- (63) Vu, D. Q.; Koros, W. J.; Miller, S. J. Mixed matrix membranes using carbon molecular sieves: I. Preparation and experimental results. *J. Membr. Sci.* **2003**, *211* (2), 311–334.
- (64) Zhang, Y.; Musselman, I. H.; Ferraris, J. P.; Balkus, K. J. Gas permeability properties of Matrimid® membranes containing the metal-organic framework Cu–BPY–HFS. *J. Membr. Sci.* **2008**, 313 (1), 170–181.
- (65) Luo, S.; Wiegand, J. R.; Gao, P.; Doherty, C. M.; Hill, A. J.; Guo, R. Molecular origins of fast and selective gas transport in pentiptycene-containing polyimide membranes and their physical aging behavior. *J. Membr. Sci.* **2016**, *518*, 100–109.

- (66) Koros, W. J.; Fleming, G. K.; Jordan, S. M.; Kim, T. H.; Hoehn, H. H. Polymeric membrane materials for solution-diffusion based permeation separations. *Prog. Polym. Sci.* **1988**, *13* (4), 339–401.
- (67) Puleo, A. C.; Paul, D. R.; Kelley, S. S. The effect of degree of acetylation on gas sorption and transport behavior in cellulose acetate. *J. Membr. Sci.* **1989**, *47* (3), 301–332.